Fall 2007

Consequences of fine-scale heterogeneity on predictions of the carbon cycle using lidar data and a height-structured ecosystem model

R Quinn Thomas
University of New Hampshire, Durham

CONSEQUENCES OF FINE-SCALE HETEROGENEITY ON PREDICTIONS OF THE CARBON CYCLE USING LIDAR DATA AND A HEIGHT-STRUCTURED ECOSYSTEM MODEL

BY

R. QUINN THOMAS

A.B. Dartmouth College, 2005

THESIS

Submitted to the University of New Hampshire

in Partial Fulfillment of

the Requirements for the Degree of

Master of Science

In

Natural Resources

September, 2007

UMI Number: 1447911

This thesis has been examined and approved.

Thesis Director, George C. Hurtt, Associate Professor of Natural Resources and Earth, Oceans, and Space

John D. Aber, Professor of Natural Resources and Earth, Oceans, & Space,

Scott V. Ollinger, Assistant Professor of Natural Resources and Earth, Oceans, and Space

Ralph O. Dubayah, Professor, Department of Geography, University of Maryland, College Park, MD

K. Jon Ranson, Head, Biospheric Science Branch, Code 614.4, NASA Goddard Space Flight Center

26 July '07

Date

ACKNOWLEDGEMENTS

Thank you to:

George Hurtt and my committee, John Aber, Ralph Dubayah, Scott Ollinger, and Jon Ranson, for excellent scientific guidance and support.

NASA – UNH Research and Discover Fellowship and the UNH Travel Grant for financial assistance

In no particular order, Cary Girod, Matt Fearon, Jeremy Fisher, Justin Fisk, Shannon Rogers, Mariya Schilz, and Paul Schwarz for data, assistance and/or insight during various stages of this project

Cayelan Carey for help and support throughout.

And finally, my parents, Jane and Frank Thomas, for all their support prior to and during my journey at UNH

Some data used in this thesis were obtained by scientists of the Hubbard Brook Ecosystem Study; this thesis has not been reviewed by those scientists. The Hubbard Brook Experimental Forest is operated and maintained by the Northeastern Research Station, U.S. Department of Agriculture, Newtown Square, Pennsylvania.

TABLE OF CONTENTS

LIST OF FIGURES

ABSTRACT

CONSEQUENCES OF FINE-SCALE HETEROGENEITY FOR PREDICTIONS OF THE CARBON CYCLE USING LIDAR DATA AND A HEIGHT-STRUCTURED ECOSYSTEM MODEL

by

R. Quinn Thomas

University of New Hampshire, September, 2007

To more accurately predict carbon stocks and fluxes in forests, it is important to measure fine-scale heterogeneity in ecosystem structure across the landscape, and incorporate the underlying mechanisms responsible for the observed heterogeneity in ecosystem models. This study used large-footprint lidar and a height-structured ecosystem model to estimate carbon stocks and fluxes at Hubbard Brook Experimental Forest (HBEF). At HBEF elevation gradients yield a decline in aboveground carbon stock, due to changes in net growth rates and disturbance at higher elevations. Lidar and a height structured ecosystem model can accurately quantified aboveground carbon stocks. Estimates of aboveground carbon fluxes depended on the availability of lidar data, the representation of fine-scale heterogeneity in climate and soil inputs, and the simulation of spatial variation in disturbance. Predictions of forest

structure depended strongly on simulating the mechanisms that drive heterogeneity in forest structure across the landscape.

CHAPTER I

INTRODUCTION

For predictions of carbon flux in forest ecosystems to be accurate it is important to measure the heterogeneity in ecosystem structure across the landscape and to incorporate the mechanisms responsible for this observed heterogeneity in ecosystem models (Donoghue 2002). If spatial data on heterogeneity in forest ecosystem structure is lacking, it is only practical to assert that the actual structure is contained in bounds delimited by the structure of a young secondary forest and the structure of a mature forest. For carbon research, these bounds can represent a large range of carbon stocks and fluxes, as carbon stocks increase and carbon fluxes decrease substantially through forest succession (Shugart 1984).

Constraint of landscape estimates of carbon stocks and fluxes can be provided through direct measurement of ecosystem structure. Many techniques, including national forest inventories and remote sensing, are used to directly measure forest structure. Direct measurement of individual tree size in national inventories is a highly accurate way to quantify aboveground carbon stocks and flux (Gillespie 1999, Goodale et al. 2002), but inventory data is limited in some regions and standardization of field protocols is a challenge. To overcome this limitation, the remote sensing community is measuring ecosystem structure and aboveground carbon stocks without the geographic constraints of inventory data using optical (Dong et al. 2003), radar (Kasischke et al. 1997), and laser sensors (Lefsky et al. 2002b).

Exciting progress has been made mapping ecosystem structure with high accuracy, especially canopy height and aboveground carbon stocks, using lidar remote sensing (Dubayah and Drake 2000, Lefsky et al. 2002b). At spatial resolutions that range from sub-meter to kilometers, lidar (light detection and ranging) measures vegetation structure by actively emitting pulses of laser energy toward the earth surface using airborne or space-based instruments. The distance from the sensor to structural elements on the surface (i.e., tree canopies or the ground surface) is measured using the time required for light from the object to return to the lidar sensor. Canopy height is calculated by comparing earlier returns to ground returns. Small-footprint lidar (< 1m resolution) can accurately represent very fine-scale heterogeneity in the height and biomass of individual trees (Popescu et al. 2003, Clark et al. 2004, Patenaude et al. 2004, van Aardt et al. 2006), but the high data density can limit the spatial scale of research. Large footprint lidar technology (25-250m footprints), namely the airborne Laser Vegetation Imaging Sensor (LVIS: Blair et al. 1999) and space-borne ICESat (Zwally et al. 2002) instruments, measures canopy height across regional and global scales (Peterson 2000, Drake et al. 2002, Lefsky et al. 2002a, Anderson et al. 2006). Large-footprint lidar canopy height measurements are shown to correlate well with forest aboveground carbon stocks across many different forest types (Drake et al. 2002, Lefsky et al. 2002a, Anderson et al. 2006), and to improve predictions of carbon fluxes by serving as initial conditions for ecosystem models (Hurtt et al. 2004). Lidar technology will likely continue as an important component of forthcoming carbon research, as demonstrated by the prominent position of the technology in the 'decadal survey' for earth observing satellites by the U.S. National Academies (Space Studies Board 2007).

Beyond measurements of ecosystem structure, estimates of carbon flux also require an understanding of the underlying mechanisms that explain the heterogeneity in ecosystem structure. Figure 1 illustrates an intuitive example where a stand is shorter (stand A) than the stands that surround it (Figure 1a). A suite of potential mechanisms could explain why stand A is shorter than the surrounding stands. The short stand could be a

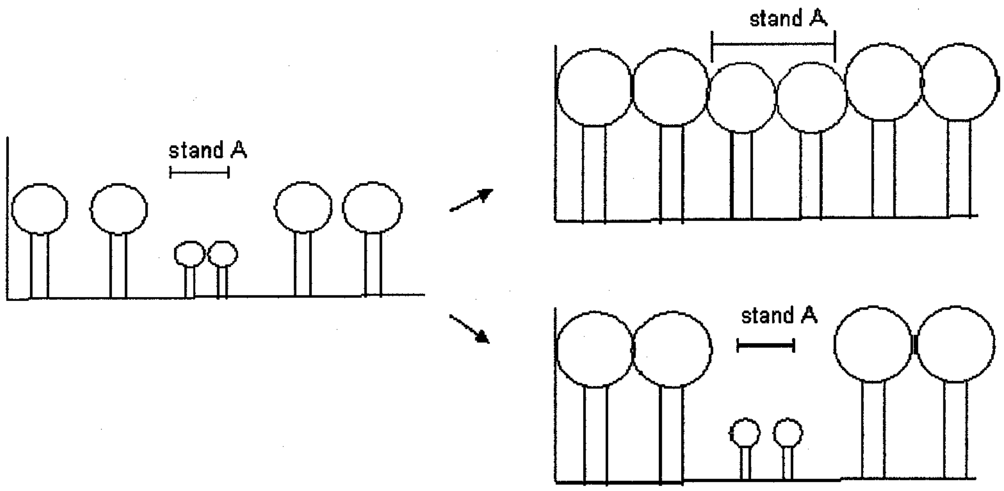

Figure 1. A schematic that illustrates how different mechanisms explaining similar heterogeneity in forest structure can yield different predictions of change (a) Heterogeneous forest structure with a stand (stand A) that has a shorter statue than surrounding stands at time *t*. (b) Forest structure at time *t*+1 when a recent disturbance is responsible for the short statue in stand A at time *t*. (c) Forest structure at time *t*+1 when locally harsh environmental conditions that constrain net growth rates are responsible for the short statue of stand A at time *t*. Examples of forest structure (y-axis) include canopy height and aboveground carbon stocks.

function of locally harsh environmental conditions that constrain growth and thus little change in structure is expected between time t and t + 1 (Figure 1b). In contrast, a disturbance event may have reset the height of the stand more recently than the surrounding stands and the structure is expected to grow quickly (Figure 1c). As this example demonstrates, the mechanisms that govern the heterogeneity in ecosystem structure can have important implications for on forest structure dynamics and the associated carbon flux

A variety of modeling techniques are utilized to simulate the mechanisms that govern heterogeneity in ecosystem structure and aboveground carbon stocks. Two dominant classes of models that simulate forest ecosystem structure dynamics are gap models and more aggregated ecosystem models. Gap models explicitly represent many aspects of forest structure, particularly canopy height, and have traditionally focused on modeling the heterogeneous nature of disturbance recovery along with the corresponding heterogeneity in light environments (Botkin et al. 1972, Shugart and West 1977, Shugart 1984, Pacala et al. 1993, Pacala et al. 1996). More aggregated ecosystem models, such as the TEM (Raich et al. 1991, Melillo et al. 1993) and IBIS (Foley et al. 1996) models, focus on physiologically-driven carbon dynamics at large spatial scales. As a link between gap and more aggregated ecosystem models, physiologically-driven forest gaps models integrate the community dynamics in forest gaps models with the physiological-based carbon dynamics found in more aggregated models to simulate the contribution of individual tree growth and mortality to the carbon cycle. Key examples of physiologically-driven forest gap models include the Hybrid (Friend et al. 1997) and the Ecosystem Demography model (ED: Hurtt et al. 1998, Moorcroft et al. 2001)

There is a growing body of studies that use remote sensing as inputs to ecosystem process models, including reviews on the subject (Lucas and Curran 1999, Turner et al. 2004). Remote sensing data can be used to estimate model variables or to reparameterize models following data assimilation, but commonly remote sensing inputs serve as initial conditions for the model simulations (Lucas and Curran 1999). For example, Hurtt et al. (2004) used lidar canopy height data to initialize the height-structured ED model and estimate aboveground carbon stocks to within 1.2% of the field estimate at the La Selva Biological Station, Costa Rica. Lidar data were also shown to provide substantial constraints on model estimates of carbon fluxes from 0.0 – 0.4 to 0.04 – 0.08 kg $C \cdot m^{-2} \cdot yr^{-1}$. In this system dominant variation in carbon stocks and fluxes was suggested to be due to disturbance. In contrast, a study by Ranson et al. (2001) used remote sensing to initialize a forest gap model in a northern forest ecosystem where growth rates depended on variations in soil characteristics. The authors used spatial maps of soil type and radar measurements of forest structure (Ranson et al. 1997) to initialize soil characteristic-specific model simulations. In the study, predictions of carbon fluxes depended strongly on both the ability to initialize the model with radar carbon stocks measurements and to resolve the mechanism through which soil type influences forest development.

Forest structure and carbon flux in the most complex environments depend on variation in historical disturbance, future disturbance, and both soil and climate constraints on growth rates across the landscape. Regions with high topographical variation are notable examples of ecosystems where the influence of disturbance, climate, and soil characteristics interact to yield heterogeneity in forest structure and fluxes that depend strongly on elevation (Whittaker and Niering 1975, Singh et al. 1994, Gerhardt and Foster 2002, Joshi et al. 2003). Hubbard Brook Experimental Forest (HBEF; Figure 2), New Hampshire (USA) is an example of an ecosystem with topographically dependent variation in forest growth and disturbance rates that contribute strongly to heterogeneity in aboveground carbon stocks (Figure 3), canopy height (Figure 4), and

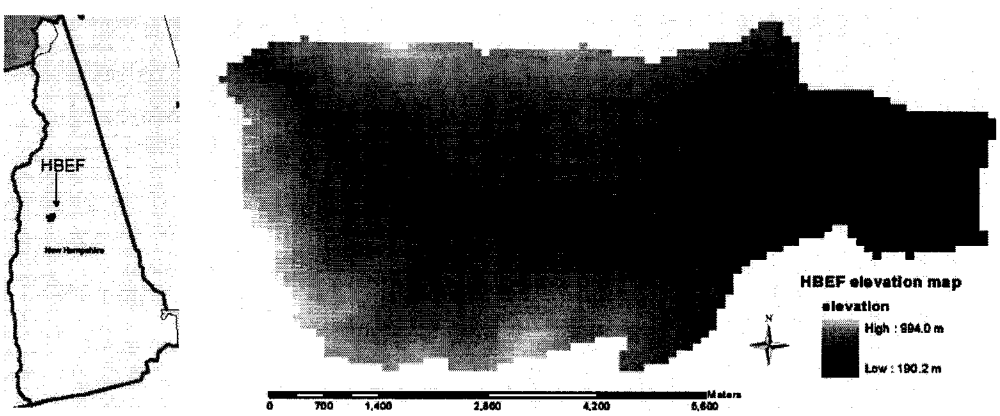

Figure 2. (a) The location of Hubbard Brook Experimental Forest (HBEF) in New Hampshire, USA. (b) A map of ground elevation at HBEF measured by the Laser Vegetation Imaging Sensor (LVIS).

forest structure in general (Bormann et al. 1970). In particular, mean aboveground carbon stocks decline by 44% (Figure 3) and canopy height declines by 39% (Figure 4) between 300 and 900m elevation (Fahey et al. 2005, Schilz 2006). This decline in aboveground carbon stocks can be explained using direct and indirect environmental influences, with the partitioning between gradients in forest growth and disturbance serving a fundamental distinction between influences. Schilz (2006), using measurements of plot age, partitioned the mechanisms responsible for the pattern of aboveground carbon stocks at HBEF, with 60% of the total decline due to decreased net growth rates (growth minus non-plot age resetting mortality) and 40% due to increased disturbance (plot age resetting mortality) at higher elevations. The 60% decrease in net growth rates is likely due to colder temperatures, shorter growing seasons, and decreased soil depth at higher elevations (Bormann et al. 1970, Schilz 2006). The increase in disturbance at higher elevation likely includes gradients in regularly occurring disturbance (i.e., wind throw of indvidual trees, Bormann et al. 1970), semi-regular disturbance (i.e., ice storm and hurricanes, Rhoads et al. 2002), and non-reoccurring disturbance (i.e., logging, Peart et al. 1992) with elevation, although studies have not partitioned the 40% increase in disturbance between these different disturbance regimes.

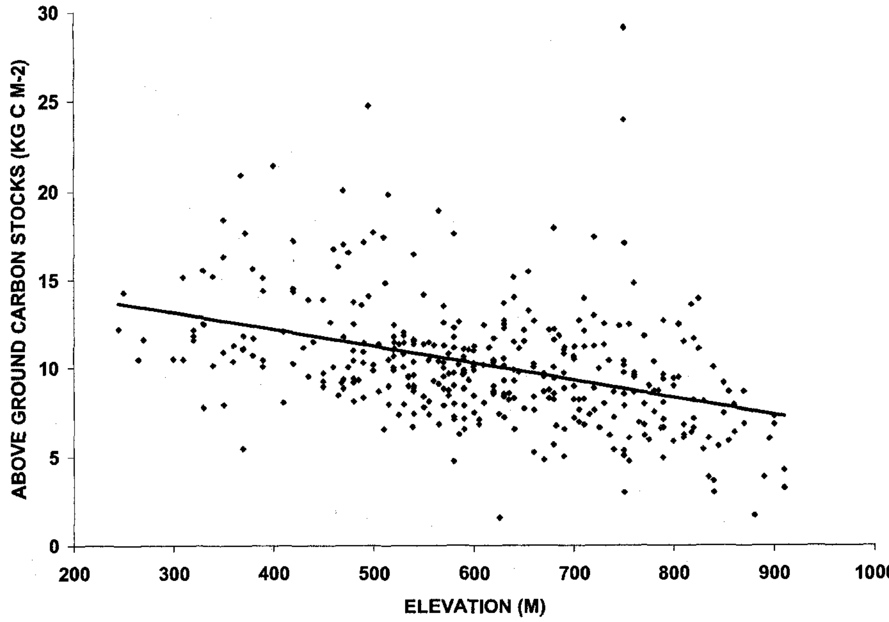

Figure 3. Aboveground carbon stocks for 371 field plots as a function of elevation at Hubbard Brook Experimental Forest (Fahey et al. 2005)

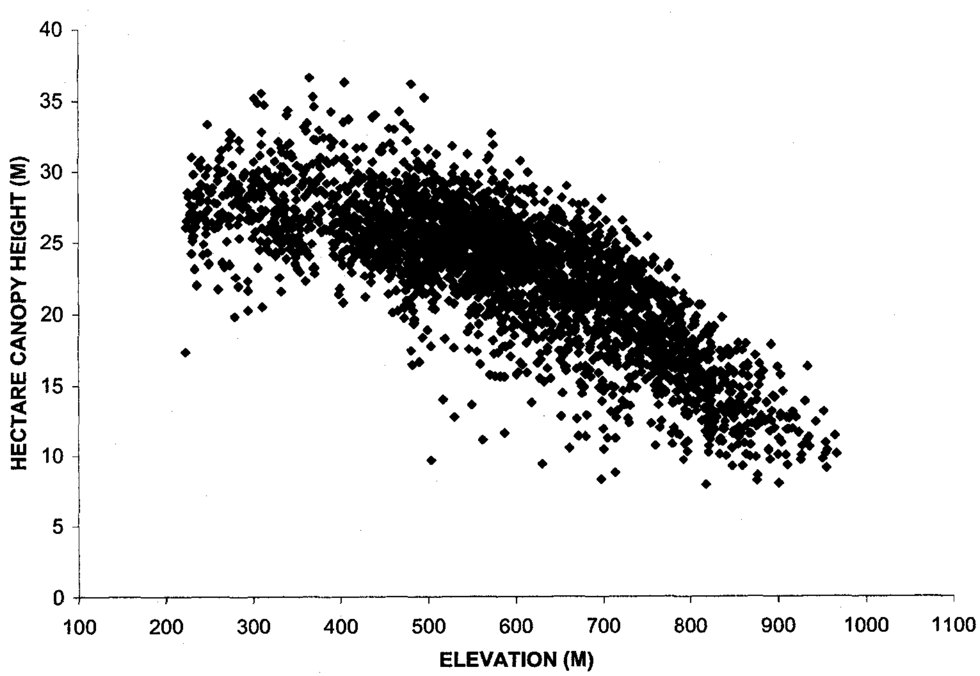

Figure 4. Lidar measured canopy height (1 hectare resolution) as a function of elevation at the Hubbard Brook Experimental Forest.

In this study, we investigated the use of lidar data and the ED model as an effective tool for estimating carbon stocks and fluxes in an environment where variation in climate, soil characteristics, and disturbance influences the spatial patterns in forest structure. We use HBEF as a case study for three primary reasons: one, to extend of results in Hurtt et al. (2004) to a temperate system; two, the mechanisms that determine patterns of carbon stocks and fluxes include heterogeneity in both net growth rates and disturbance recovery; and, three, the extensive field studies at HBEF provide important data to understand the underlying explanatory mechanisms and validate estimates. We then assess the sensitivity of carbon stocks and flux estimates to three key components: the availability of lidar data for initial conditions, the availability of elevation resolved climate and soil inputs, and assumptions about how disturbance scales with elevation.

CHAPTER II

METHODS AND RESULTS

Study Area, Data, and Model

Hubbard Brook Experimental Forest (HBEF) (44.56N, 71.45W) is located in the White Mountains of New Hampshire (USA) and is a well-studied 3076 hectare domain within a northern hardwood and spruce-fir-birch transition forest ecosystem (Figure 2a). HBEF is a bowl-shaped basin with elevations that range from 222 to 1015m (Figure 2b). While HBEF is most recognized for watershed level research (Whittaker et al. 1979, Likens and Bormann 1995), extensive basin-wide forest structure data, including diameter at breast height (DBH), canopy height (height of the three tallest trees), and carbon stocks, are available from 371 500-m^2 basin wide permanent plots measured between 1995 and 1997 (Schwarz et al. 2003).

The HBEF has a history of land-use and natural disturbance that has shaped the present day ecosystem structure and function. Natural disturbance includes regularly occurring wind-throw(Bormann and Likens 1979), a hurricane in 1938(Merrens and Peart 1992, Peart et al. 1992), and an ice-storm in 1998 (Rhoads et al. 2002). Land-use includes valley-wide logging in the early 1900's that paralleled the distribution of red spruce (Peart et al. 1992) and approached clear cutting is some areas. Additional salvage logging occurred following the 1938 hurricane (Peart et al. 1992). Recently, whole watershed have been experimentally harvested, with tree removal ranging from strip cutting to a total harvest followed by three years of vegetation suppression.

In June 1999, ecosystem structure data was collected over the Northeastern United States, including HBEF, using NASA's Laser Vegetation Imaging Sensor (LVIS). The mission was flown at an altitude of ~8km with a nominal footprint size of 25 m diameter. Footprints were spaced every ~9 m across track, for a total swath width of 1 km, and were spaced ~27m along track, for approximately contiguous coverage. The return waveform was digitized at 60 cm vertical increments allowing a detailed description of canopy vertical structure. For the purposes of this study, the first return (canopy height) and the ground return (ground elevation) for each 25 m footprint were aggregated to 1 ha resolution.

Ecosystem dynamics were simulated using the Ecosystem Demography model (Hurtt et al. 1998, Moorcroft et al. 2001), a height-structured mechanistic forest-gap type ecosystem model driven by sub-models that govern forest processes (i.e., growth, reproduction, dispersal, respiration, mortality, etc). The ED model statistically scales up forest dynamics, allowing scales ranging from local sites to the globe to be computationally practical. The general nature of the model has been applied in many different ecosystems, including the Amazon (Moorcroft et al. 2001), the coterminous United States (Hurtt et al. 2002, Albani et al. 2006), and Costa Rica (Hurtt et al. 2004).

The ED model used in this study underwent minor refinements for application to the northern hardwood ecosystem at HBEF. First, two northern hardwood plant functional types were parameterized in the model using two allometries described in Whittaker et al. (1974) and Siccama et al. (1994): a hardwood allometry, represented by using the American beech (*Fagus grandifolia* Ehrh) allometry, and a red spruce (*Picea rubens* Sarg.) allometry. The similarity in allometry between the three dominant hardwood species at HBEF allowed a single species to represent the two other species (Whittaker et al. 1974). Secondly, the temporal resolution was increased from a monthly time-step to a weekly time-step to allow sub-monthly gradients in growing season length. Thirdly, the temperature threshold marking spring leaf out and fall leaf drop, as described in Hurtt et al. (2002), was decreased from 10°C to 8.5°C so that the predicted total growing season days matched the relationship

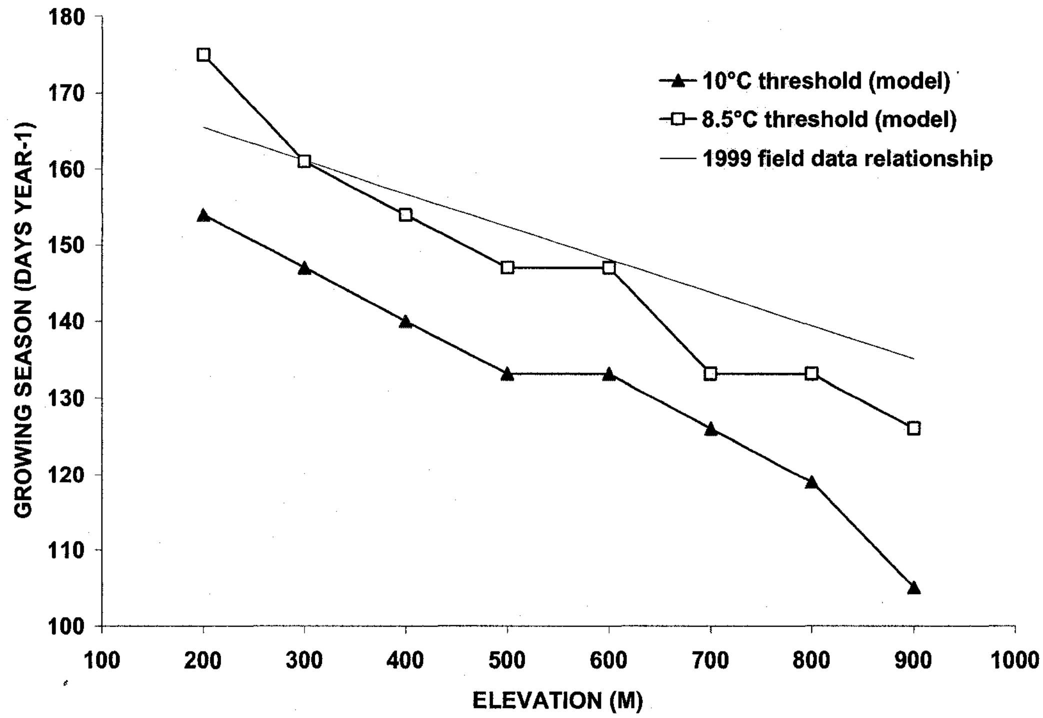

Figure 5. Number of days during 1999 with complete leaf coverage as a function of elevation. Field estimates were collected through routine observations of a sample of individual trees (Bailey 2001). Model estimates are from the phenology sub-model in the Ecosystem Demography Model using the updated leaf on, leaf off threshold of 8.5°C. The model estimates using the original 10°C threshold used in Hurtt et al. (2002) are shown for reference.

between phenology and elevation in field data collected in 1999 at the HBEF (Bailey 2001, Schilz 2006) across the elevation gradient at HBEF (Figure 5). Finally, the regular disturbance rate parameter was set to 0.70% per year across all elevations. All other sub-models described in Moorcroft et al. (2001) and Hurtt et al. (2002) were not altered.

The ED model predicts ecosystem dynamics using only climate and soil data as inputs, both of which were collected at HBEF and scaled with elevation to cover all elevations. Specifically, hourly temperature, photosynthetically active radiation (PAR), and relative humidity were collected between 1982 and 1999 at the HBEF headquarters weather station located at an elevation of 250m and organized in a weekly climatology. Temperature was scaled to decrease with elevation using the adiabatic lapse rate (6.5° per km) and precipitation was scaled to increase with elevation using the linear equations described in Ollinger et al. (1995). PAR and relative humidity were assumed to be constant over all elevations, consistent with Richardson et al. (2004). Soil texture inputs were equivalent to the inputs described in Hurtt et al. (2002) and soil depth inputs linearly scale from 467mm at 300m elevation to 233mm at 900m elevation, as described in Schliz (2006). The elevation dependent climate and soil characteristics inputs were aggregated into seven 100m resolution elevation bands ranging from 200 to 1000m elevation.

Estimating Carbon Stocks and Fluxes

The climate data was used as input into the ED model and forest development over 500 years was simulated using the inputs specific to each elevation band. Model output from each elevation specific simulation was organized into a look-up table that used canopy height to index the corresponding aboveground carbon stocks and flux output. The height-based organization of forest structure aided initialization using lidar canopy height measurements.

Before using lidar data to initialize the canopy height in the ED model and estimate carbon stocks and fluxes, we compared the relationship between canopy height and carbon stocks in the model to the same relationship in the field. The carbon stocks increased nearly linearly across the range of heights measured in 371 field plots between 1995 and 1997 (Figure 6). The model relationship also increased linearly with no significant difference from the slope and intercept of the field data (model estimate contained in the field 95% confidence intervals; Figure 6). Furthermore, the ED-based relationship between canopy height and carbon stocks was constant across all elevations. The close agreement between the carbon-height relationship in the field and in the model serves as a partial validation of the model representation of forest structure. We did not observe an early asymptote in the height versus carbon relationship at 29m that was demonstrated using the same model at La Selva Biological Station in Costa Rica – likely due to differing allometric relationships (Hurtt et al 2004).

Building on the close correspondence between field and ED-based estimates, we next initialized the canopy height in the ED model and estimated aboveground carbon stocks using the 1 ha map of canopy height and elevation, and compared the domain wide and elevation patterns of carbon stocks to field measurements (Figure 7). Aboveground carbon stocks for each hectare across the HBEF domain was estimated by

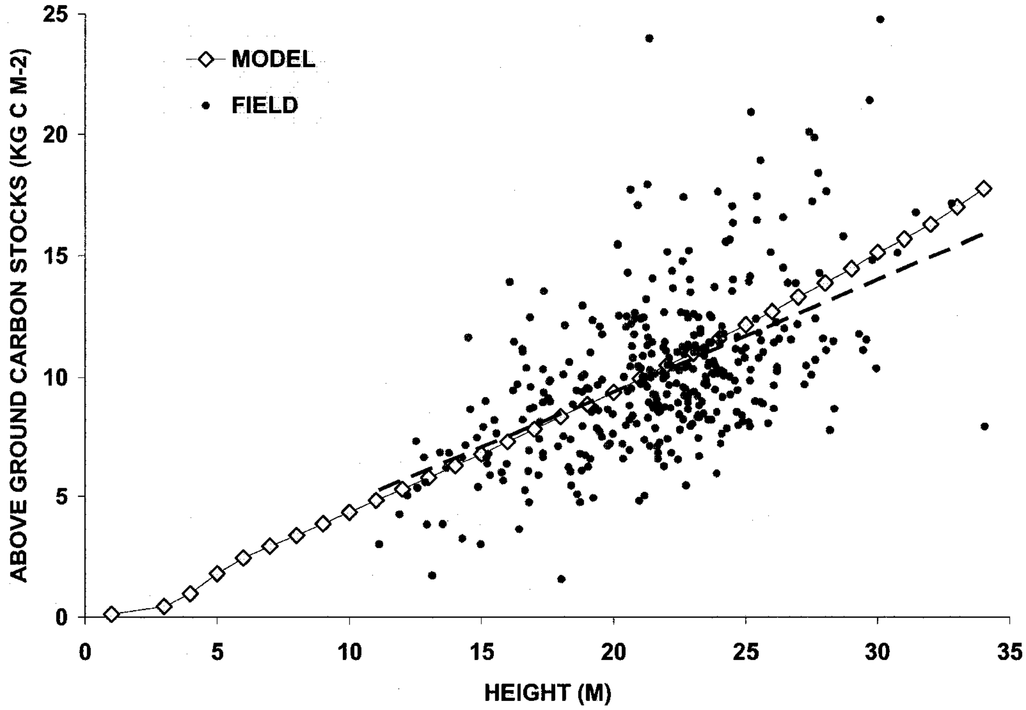

Figure 6. Aboveground carbon stocks as a function of canopy height, predicted by the Ecosystem Demography model (white diamonds) and measured in the field (gray circles with a dotted line showing the linear best fit; Schwarz *unpublished data*).

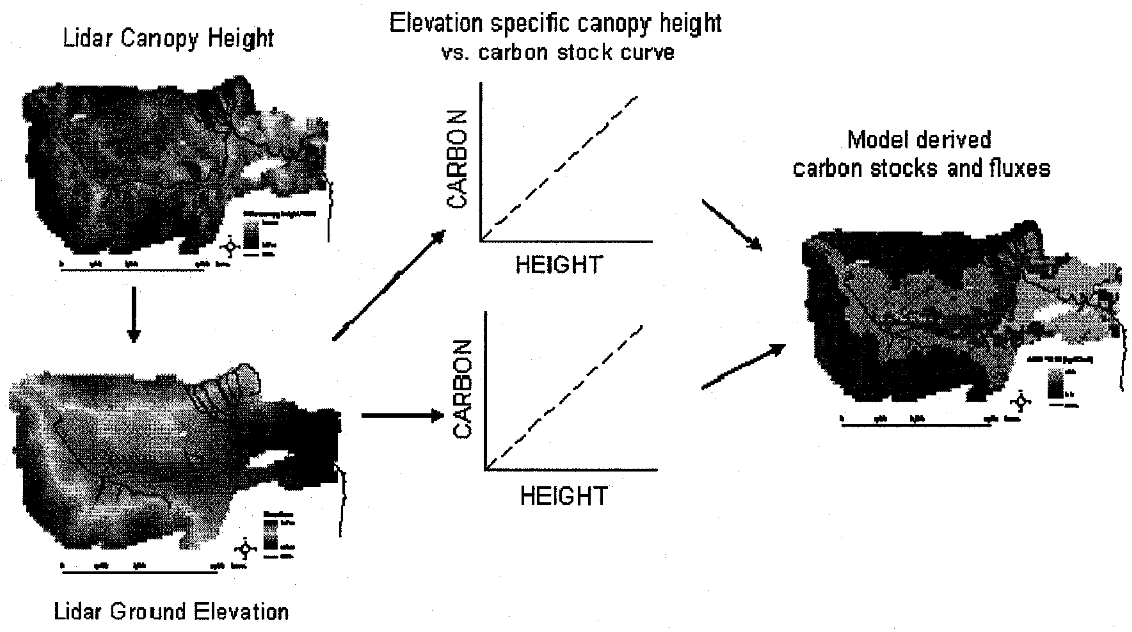

Figure 7. Schematic of the methodology used to estimate carbon stocks using the Ecosystem Demography model, lidar canopy height, and lidar ground elevation measurements. The ground elevation measurements were used to reference the corresponding elevation-specific canopy height versus aboveground carbon stocks look-up table. Carbon stocks were estimating using lidar canopy height to index the height/carbon stock relationship. A similar methodology was used to estimate carbon fluxes.

first using the elevation map to reference the corresponding elevation specific look-up table that relates simulated carbon stocks to canopy height. Then, the lidar canopy height for the same hectare was used to index to the corresponding carbon stocks.

There was close correspondence between domain wide mean and elevation pattern in field and lidar initialized aboveground carbon stocks.

Specifically the domain wide mean initialized carbon stocks (10.77 ± 0.12 kg C · m^{-2}) were within 5.4% of the field data (10.17 ± 0.35 kg C · m^{-2}). There was also close agreement between the field and lidar initialized elevation patterns in carbon stocks. The lidar initialized carbon stocks showed a 45% decline from 300 to 900m elevation, a result similar to the 44% decline measured in the field. Figure 8 shows a spatial distribution of aboveground carbon stocks. Both elevation and recent land-use patterns (i.e. experimental tree harvest) are clearly visible in Figure 8.

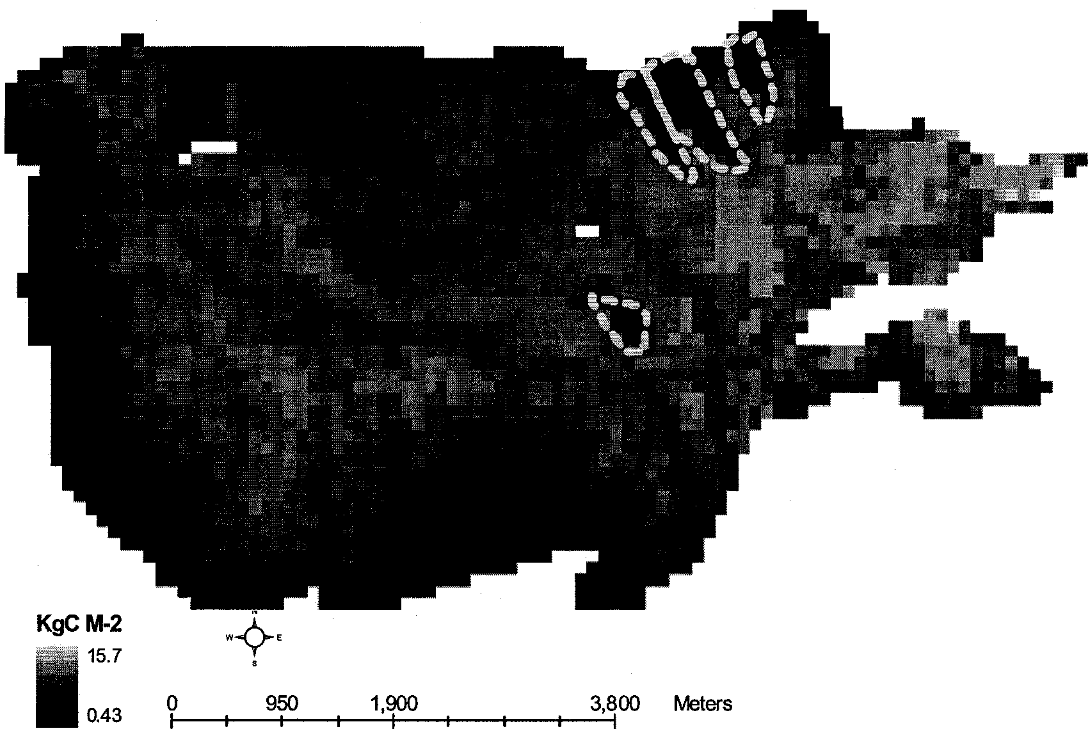

Figure 8. A map of estimated aboveground carbon stocks at Hubbard Brook Experiment Forest. Lidar canopy height and ground elevation data was used to initialize the Ecosystem Demography model. Tree harvest has occurring since the 1950s in the outlined watersheds.

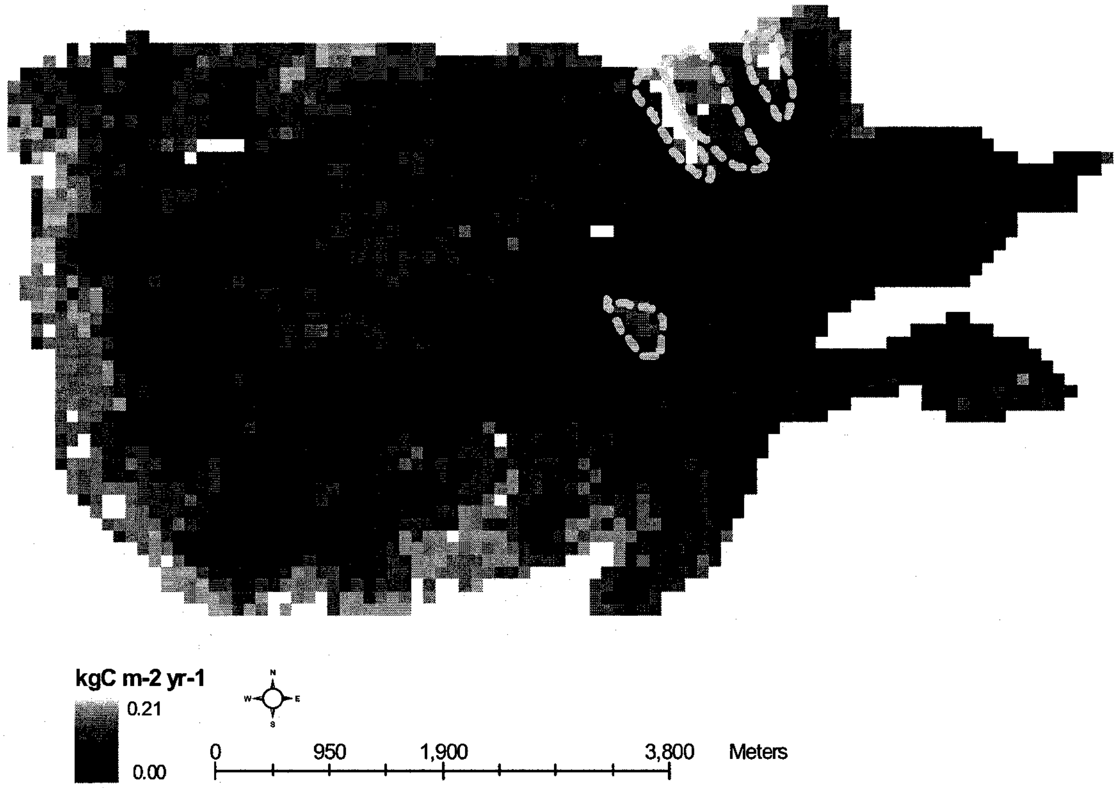

Figure 9 A map of estimated aboveground carbon fluxes at Hubbard Brook Experiment Forest. Lidar canopy height and ground elevation data was used to initialize the Ecosystem Demography model. Tree harvest has occurring since the 1950s in the outlined watersheds.

We used lidar canopy height and elevation data and the ED model to produce spatial maps of aboveground carbon flux. The carbon fluxes were determined using the same elevation specific canopy height index technique used to estimate carbon stocks. Estimates of carbon flux represent an average annual flux that corresponded to the average climatic conditions between 1981 and 1999. Figure 9 shows a spatial map of carbon fluxes. Relatively high carbon fluxes are present in the outlined experimental watersheds, but overall the carbon flux across the domain was near zero. The estimated mean carbon flux across HBEF was 0.023 ± 0.001 kg C m^{-2} y^{-1}.

Sensitivity to Major Factors

Next, we tested the sensitivity of the results described above to key inputs and assumptions: the availability of 1-ha resolution lidar data, the availability of elevation resolved climate and soil input, and the assumption that the regular disturbance rate does not increase with elevation.

To illustrate the importance of lidar data, we estimated the range of uncertainty created when lidar or other high-resolution, spatially continuous, measurements of forest structure or succession were unavailable. This exercise was prudent given the need for regional to global predictions of carbon dynamics combined with the limited availability and non-random distribution of airborne LVIS data and field data (i.e. LTER sites). Specifically, we used two scenarios to bracket the range of uncertainty in estimated carbon stocks and fluxes when lidar was unavailable. First, we assumed that the entire HBEF domain was early in

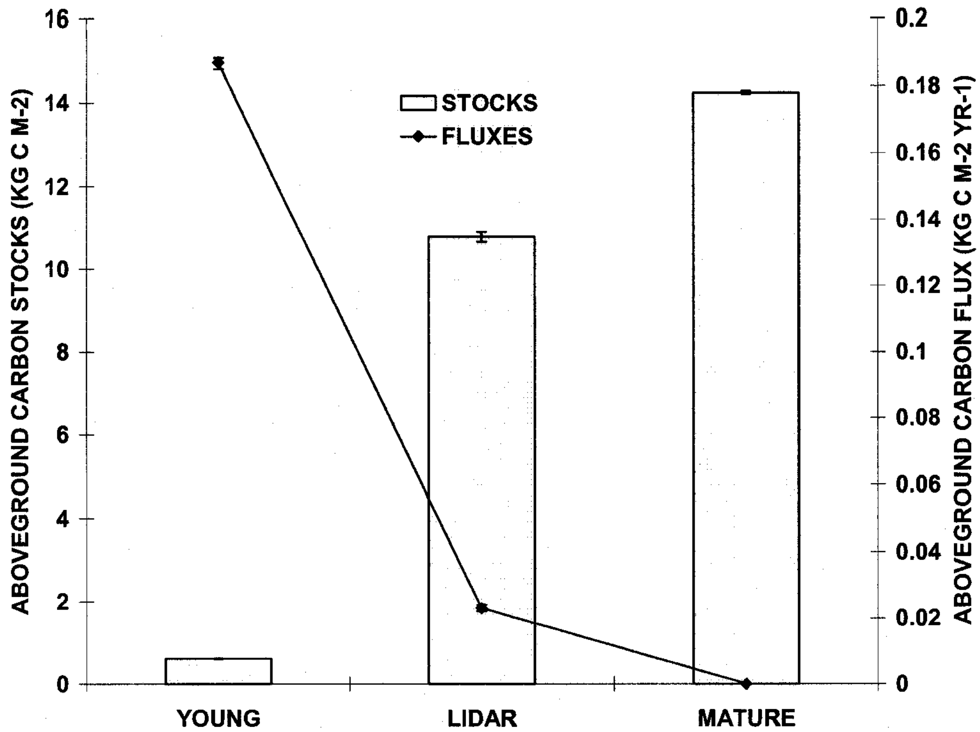

Figure 10. Estimates of domain wide mean aboveground carbon stocks (bars) and fluxes (line). Lidar based estimates used canopy height data for initialization. The Young and Mature estimates used assumptions that the entire domain is early or late in succession, respectively, and brackets the uncertainty when lidar is unavailable. Simulation included elevation patterns in environmental and homogeneous regular disturbance across all elevations. All error bars are ± 95% C.I.

succession (10 years old) and quickly aggregated carbon into living biomass. Second, we assumed the domain was entirely mature forest and near carbon balance, similar to the potential vegetation assumptions used as initial conditions in other modeling studies (see Melillo et al. 1993, Potter et al. 1998). In the absence of lidar data, estimated carbon stocks ranged from 0.62 kg C $\cdot$ m^{-2} to 14.24 kg C $\cdot$ m^{-2} and carbon fluxes ranged from 0.0 kg C $\cdot$ m^{-2} to 0.19 kg C $\cdot$ m^{-2} (Figure 10).

Next, we asked how the estimates of carbon stocks and fluxes changed when elevation resolved climate and soil input were not available. Our ability to resolve the elevation pattern in temperature, precipitation and soil depth inputs rested on the availability of an elevation map and empirical studies establishing the relationship between elevation and the inputs. Beyond the well-studied landscapes like HBEF, an understanding of how climate or soil varies across the landscape may be limited, despite considerable variation in forest structure. Furthermore, especially in large scale studies, climatic inputs and soil characteristics are often assumed to be homogeneous, even at scales larger than HBEF. How detrimental would such assumptions of homogeneity across an environment as heterogeneous at HBEF be to estimates of the carbon cycle? To test the sensitivity, we estimated the carbon stocks and fluxes using simulations where temperature, precipitation, and soil depth were assumed constant across all elevations. Lidar canopy height data were used to initialize each hectare by indexing the height-carbon relationship assuming all elevations were equivalent to that of the 300m elevation band.

Aboveground carbon stocks estimates varied little whether elevation dependent input were used or not; however, aboveground carbon flux estimate varied considerably (Figures 11 and 12). Aboveground carbon stock estimates without elevation dependent climatic and soil inputs (10.92 ± 0.11 kg C $\cdot$ m^{-2}) were within 1.4% of the estimates

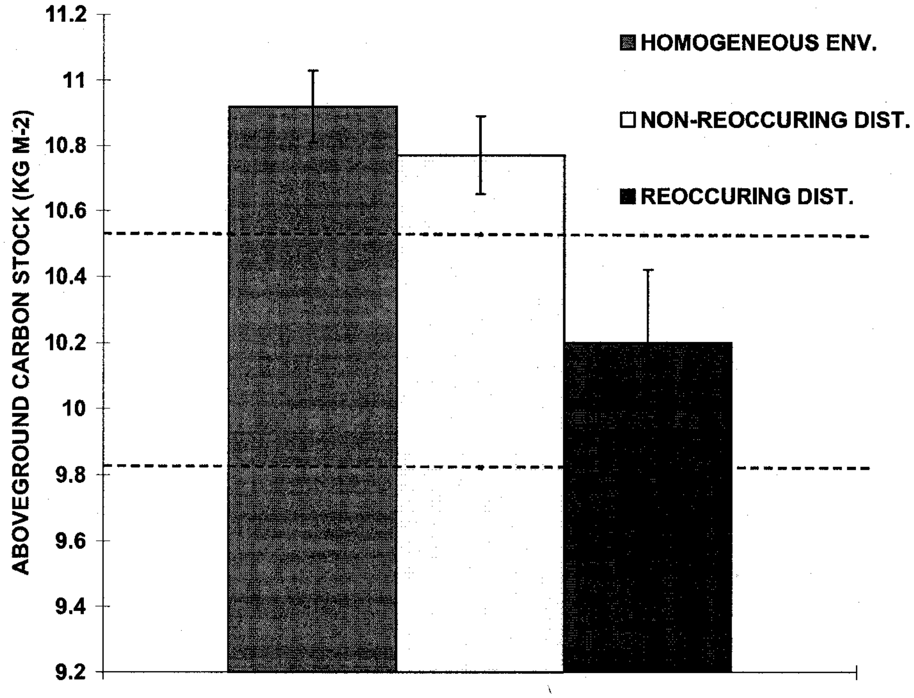

Figure 11. Estimates of domain wide mean above carbon stocks from the sensitivity analysis. All estimates use the ED-lidar look-up table method to initialize canopy height and estimate carbon stocks. Climate inputs, soil inputs, and reoccurring disturbance were constant across all elevation in the "homogenous env." simulation. Climate and soil inputs vary with elevation in the "non-reoccuring dist." and "reoccurring dist." simulations. Reoccurring disturbance increases with elevation in the "reoccurring dist." simulation. The 95% confidence interval (CI) for the domain wide mean field-measured stocks is shown as dotted lines. All error bars are ± 95% C.I. around the mean.

with elevation dependent inputs and within 7.9% of the field estimate (Figure 11). The aboveground carbon stocks declined by 43% from 300 to 900m; a result similar to the decline estimated in the simulation with elevation gradients in inputs (45%) and in measured in the field data (44%). The estimates of aboveground carbon flux were 40% higher without elevation dependent inputs (Figure 12)

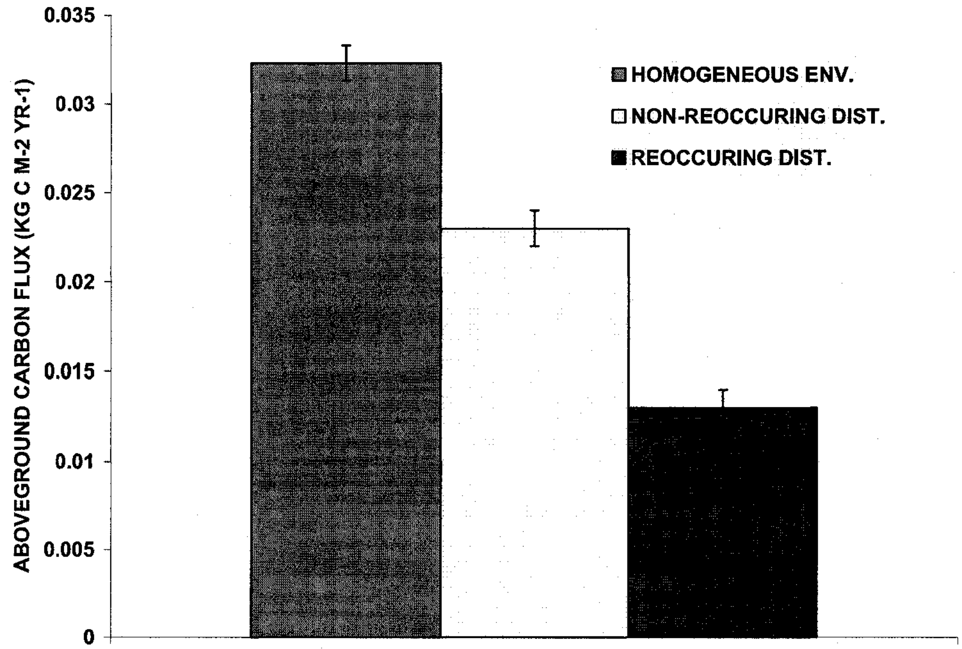

Figure 12. Estimates of domain wide mean above carbon flux from the sensitivity analysis. All estimates use the ED-lidar look-up table method to initialize canopy height and estimate carbon fluxes. Climate inputs, soil inputs, and reoccurring disturbance were constant across all elevation in the "homogenous env." simulation. Climate and soil inputs vary with elevation in the "non-reoccuring dist." and "reoccurring dist." simulations. Reoccurring disturbance increases with elevation in the "reoccurring dist." simulation. All error bars are ± 95% C.I. around the mean.

Finally, we asked how carbon stocks and flux estimates depend on assumptions about how disturbance scales with elevation. Our prior estimates of carbon stocks and fluxes assumed that the disturbance rate was a constant 0.70% per year across all elevations. In this assumption, a disturbance gradient with elevation was present but it was entirely due to historical land-use that is intrinsic to the lidar initialization. We tested the sensitivity of model estimates of carbon stocks and fluxes to assumptions about the disturbance regime by repeating the model simulation using the assumption that regular disturbance increases with elevation. This assumption required that the currently observed 44% decline in aboveground carbon stocks from 300 to 900m elevation to be a steady state property of the ecosystem. Consequently, the combination of decreased growth rates and increased regular (and recurring) disturbance with elevation, explained the observed 44% decline. This assumption precluded any gradients in land-use disturbance. We parameterized the regular disturbance rate to increase linearly with elevation by first determining the decline in aboveground carbon socks that was predicted at steady state due only to decreased net growth rates. We then used the gradient in net growth rate to solve for the additional gradient from annual disturbance that was needed to yield, at steady-state, the observed 44% (Figure 3) decline in aboveground carbon stocks from 300 to 900m. The annual disturbance rate was assumed to increase linearly with elevation using the following equation with a baseline value of 0.70% individuals per time step at 300m elevation:

$$\text{Disturbance rate} = 0.0007 + (x - b) * (8 * 10^{-6}) \quad (1)$$

where x is the elevation and b is the baseline elevation (300m). The elevation specific canopy height look-up table approach (Figure 7) was used to estimate the carbon stocks and flux using lidar data.

Lidar initialized aboveground carbon stocks were not overly sensitive to assumptions about the disturbance regime while aboveground carbon fluxes at higher elevations were much lower when regular disturbance increased with elevation (Figures 11 and 12). Lidar initialized domain wide mean carbon stocks (ranged from 10.20 to 10.77 $kgC \cdot m^{-2}$) and the pattern with elevation (ranged from 45-47% decline) were relatively insensitive to assumptions about how disturbance increases with elevation. Carbon fluxes were very sensitive to assumptions about the disturbance, as the carbon flux estimates were 43% less in the case with increasing regular disturbance (Figure 12). The carbon flux estimates that bounded contained by the two disturbance regimes (all historical versus all regularly occurring) ranged from 0.013 to 0.023 $kg\ C \cdot m^{-2} \cdot y^{-1}$.

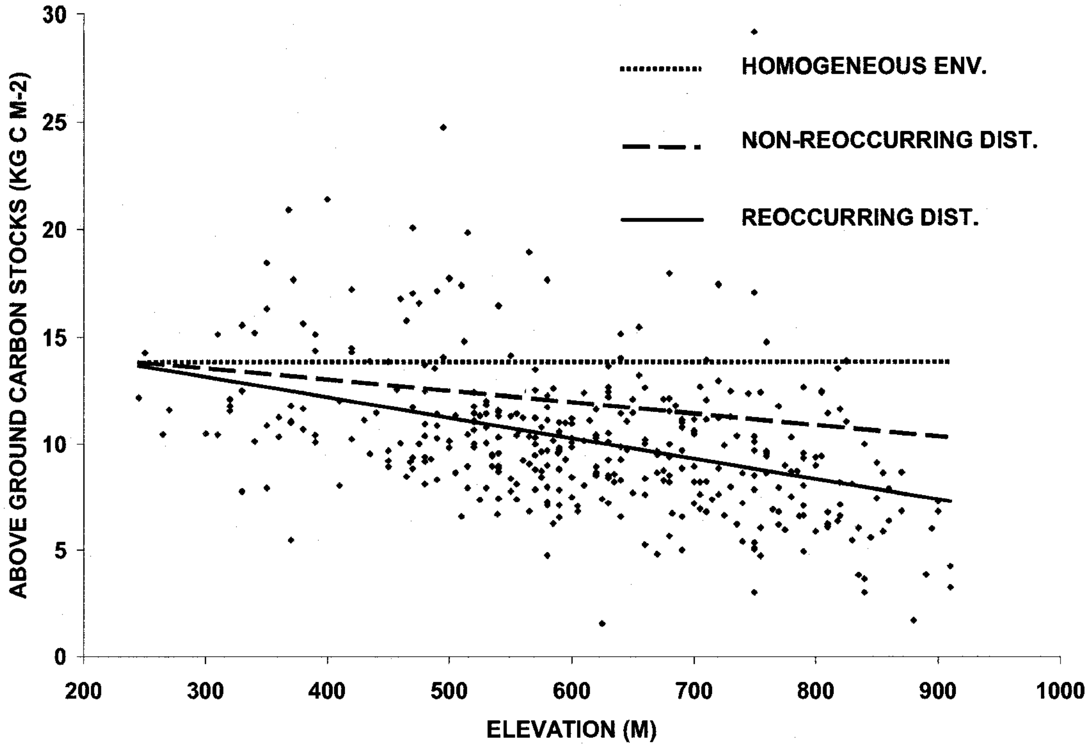

Figure 13. Elevation patterns in aboveground carbon stocks that are expected at steady state for the different sensitivity analysis simulations. The field data collected between 1995 and 1997 is shown for reference (Fahey et al. 2005).

The inclusion of environmental gradients and details on disturbance affected not only the aboveground carbon stocks and fluxes, but the implied elevation gradient of aboveground carbon stocks at steady state. Initialization with lidar data yield ~44% decline in aboveground carbon stocks from 300 to 900m, regardless of the elevation patterns in inputs or disturbance regimes; however, after simulations are allowed to continue to steady state following initialization, the cases differed substantially. The

44% decline was maintained at steady state when the climate and soil inputs and the disturbance rate vary with elevation. The 44% decline was reduced to a 24% decline when regular disturbance was held constant and climate and soil inputs were allowed to vary with elevation. Finally and trivially, carbon stocks were constant across all elevations at steady state when all inputs and the disturbance rate were constant across all elevations.

CHAPTER III

DISCUSSION

Terrestrial ecosystems are heterogeneous due to a combination of factors including edaphic patterns, climate variation, and disturbance events. Here the combination of the height-structured ED model and lidar data was used to constrain estimates of carbon stocks and fluxes in an ecosystem where both environmental constraints on growth and disturbance rates vary across the landscape. Without the availability of lidar measurements of ecosystem structure, the range of model carbon stocks and flux estimates was large. Initialization using canopy height measurements was able to substantially reduce the range of carbon stocks and fluxes estimates. Further constraint on carbon flux estimates was provided by simulating the mechanisms that are responsible for heterogeneity in ecosystem structure. In particular, simulating the elevation dependent heterogeneity in growth and disturbance allowed the delineation of short high elevation stands constrained by harsh environmental conditions (low carbon fluxes) from recently disturbed short areas (high carbon fluxes) in the low elevations. Carbon flux estimates depended strongly on simulating the underlying elevation dependent mechanisms that explain heterogeneity in ecosystem structure across HBEF.

Data on mean canopy height from an airborne large footprint lidar sensor were used to initialize the mean canopy height and all associated underlying information on the composition, size, and density of individual plants in a height structured ecosystem model. Resulting model estimates of carbon stocks were then compared to field data on domain wide average carbon stocks, and elevation patterns of carbon stocks. Estimates of carbons stocks from data on mean canopy height thus served as partial validation of the ED model in which estimates of mean canopy height and carbon stocks are the result of the dynamics of an individual-based physiologically-driven gap processes. Empirically derived allometric relationships are important in ED, but they only describe the relation between height and carbon stocks for individual trees, not the canopy as a whole.

Beyond the constraint provided by measurements of ecosystem structure provided by lidar data, carbon flux estimates depended strongly on simulating the underlying mechanisms responsible for the heterogeneity. One of the important underlying mechanisms that explain heterogeneity in ecosystem structure at HBEF is elevation pattern in growth rates. Estimates of carbon flux were nearly double when the elevation pattern in growths was not simulated using elevation dependent climate and soil depth inputs. Lidar measurements of ground elevation and empirical relationships between the inputs and elevation were central to resolving the elevation patterns. Fine-scale heterogeneity in climate and soil inputs allowed more precise estimation of successional stage by separating climate induced from disturbance induced structural heterogeneity. The constraint provided by elevation resolved climate and soil data will likely be even more important in younger landscapes with more variability in growth rates, than the relatively mature landscape at HBEF.

Another important underlying mechanism at HBEF is variation in disturbance frequency across the landscape. Carbon flux estimates were nearly as dependent on assumptions on how disturbance increases with elevation as they were dependent on the resolution of fine-scale heterogeneity in climate and soil inputs. Carbon flux was 38% lower using lidar to initialize the simulation with a positive relationship between regular disturbance and elevation than initializing the simulation with regular disturbance constant across all elevations. Despite the sensitivity, quantifying the partition in elevation dependent disturbance between regular and non-reoccurring disturbance at HBEF is unclear. Published accounts of logging (a non-reoccurring disturbance) at HBEF suggest that logging was concentrated at higher elevations (Peart et al. 1992), while research demonstrates that wind-throw (Bormann et al. 1970) and ice-storms are more common in exposed environments at higher elevations (600-750m, Rhoads et al. 2002). Furthermore, studies have shown that interactions exist between land-use and wind-throw as stands with more recent logging history had fewer impacts from the 1938 hurricane than less recently logged stands at HBEF (Peart et al., 1992). Estimates serve as bounds for the actual disturbance regime because it is likely that the actual disturbance gradient also includes semi-regular disturbances that occur less often than yearly but will occur in the future (i.e. not a non-reoccurring disturbance). Improved predictions of carbon flux depend on the development of disturbance models that simulate the reoccurrence of disturbance as a function of environmental variation and human activities.

Understanding the impact of disturbance patterns on carbon flux is even more complex than correctly partitioning regular and irregular disturbance. First, the role of sub-lethal disturbance is unclear. Sub-lethal disturbance, or the loss of leaves and branches from storm events or neighboring tree fall, is likely to parallel the increases in wind speed and storm exposure that are associated with higher elevations . This type of disturbance would materialize as decreased net growth rates rather than as increased disturbance rates, as leaf area available for photosynthesis would be reduced and photosynthate would be reallocated to repairing damage instead of added to new growth. Second, a spatial examination of carbon fluxes (Figure 10) revealed that the estimates for carbon flux are relatively large on the high elevation ridge tops and rocky outcrops, even when climate inputs, soil inputs, and regular disturbance vary with elevation. It is likely that the actual carbon flux at these high elevation locations is substantially lower, as the model does not specifically represent the unique disturbance regimes and soil characteristics at the highest elevations in HBEF (Bormann et al. 1970).

Validation of carbon flux estimates from terrestrial ecosystem models across large spatial scales is difficult without spatially intense remeasurement of ecosystem structure. In the absence of data from repeat forest census or lidar collection, direct validation of carbon flux estimates across the entire domain at HBEF is a challenge. However, our domain wide and elevation patterns are broadly consistent with values reported in other studies. Our near zero estimate for domain wide carbon flux compares well to reports that little aboveground biomass is aggregating at HBEF (Battles, personal communication) and the total carbon flux is near zero (Fahey et al. 2005). Additionally, the simulated decline in carbon stocks with elevation due only to growth rates decreasing with elevation (24% from 300 to 900m) compares well with the corresponding decline (also 24%) measured using aboveground carbon stocks and plot age (Schilz 2006; although the study does not present uncertainty bounds around the estimates derived from highly variable data). The comparison of the growth decline predictions suggests that the elevation patterns in climate and soil inputs provide good constraint on patterns of carbon flux at HBEF.

Even with accurate initialization of forest structure, long term predictions of ecosystem dynamics require the fine-scale heterogeneity in climate and soil inputs and understanding how disturbance varies across the landscape. In all simulations, the lidar initialized carbon stocks decline equally from 300 to 900m; however, without heterogeneity in climate and soil inputs and disturbance rates, the current decline in carbon stocks from 300 to 900m is predicted to level out over time. In contrast, the decline is predicted to stay constant when climate, soil, and disturbance vary with elevation. This study shows that, in order to obtain accurate estimates of carbon stocks and fluxes simultaneously, data on ecosystem structure must be combined with models that accurately resolve the underlying mechanisms responsible for heterogeneity in ecosystem structure.

CHAPTER IV

CONCLUSIONS

The integration of height-structured ecosystem models and lidar canopy height measurements is a promising combination for improving carbon predictions in many different forest ecosystem types, especially when supplementary data (i.e. elevation maps or soil type maps) are available to aid in simulating the fine-scale variation in environmental conditions and disturbance that influences the structure. Predictions of carbon dynamics benefit from initialization to measured heterogeneity in ecosystem structure, fine-scale heterogeneity in climate and soil inputs, and the simulation of patterns in disturbance across the landscape. Improved carbon flux predictions depend on better understanding how growth rates and disturbance vary across the landscape and improving the accuracy and spatial coverage of ecosystem structure measurements. Increased spatial coverage from space-borne lidar missions, such as ICESAT and the proposed ICESAT II and DESDynI (Deformation, Ecosystem Structure, and Dynamics of Ice) missions (Space Studies Board 2007), will prove to be a valuable asset for predictive terrestrial carbon research across the globe. The scientific community and policy makers will benefit from improved constraint on predictions of the terrestrial carbon cycle provided by measuring ecosystem structure and simulating the mechanisms responsible for heterogeneity in these measurements.

LIST OF REFERENCES

Albani, M., D. Medvigy, G. C. Hurtt, and P. R. Moorcroft. 2006. The contributions of land-use change, CO2 fertilization, and climate variability to the Eastern US carbon sink. Global Change Biology **12**:2370-2390.

Anderson, J., M. E. Martin, M. L. Smith, R. O. Dubayah, M. A. Hofton, P. Hyde, B. E. Peterson, J. B. Blair, and R. G. Knox. 2006. The use of waveform lidar to measure northern temperate mixed conifer and deciduous forest structure in New Hampshire. Remote Sensing of Environment **105**:248-261.

Bailey, A. 2001. Routine Phenology Measurements. USDA Forest Service, Hubbard Brook Experimental Forest.

Battles, J. J. 2007. A decade of biomass stability and vegetational change in Hubbard Brook Valley

Blair, J. B., D. L. Rabine, and M. A. Hofton. 1999. The Laser Vegetation Imaging Sensor: a medium-altitude, digitisation-only, airborne laser altimeter for mapping vegetation and topography. Isprs Journal of Photogrammetry and Remote Sensing **54**:115-122.

Board, S. S. 2007. Earth Science and Applications from Space: National Imperatives for the Next Decade and Beyond. The National Academies Press, Washington, DC.

Bormann, F. H., and G. E. Likens. 1979. Pattern and process in a forested ecosystem : disturbance, development, and the steady state based on the Hubbard Brook ecosystem study. Springer-Verlag, New York.

Bormann, F. H., T. G. Siccama, G. E. Likens, and R. H. Whittaker. 1970. Hubbard Brook Ecosystem Study - Composition and Dynamics of

Tree Stratum. Ecological Monographs **40**:373-&.

Botkin, D. B., J. R. Wallis, and J. F. Janak. 1972. Some Ecological Consequences of a Computer Model of Forest Growth. Journal of Ecology **60**:849-&.

Clark, M. L., D. B. Clark, and D. A. Roberts. 2004. Small-footprint lidar estimation of sub-canopy elevation and tree height in a tropical rain forest landscape. Remote Sensing of Environment **91**:68-89.

Dong, J. R., R. K. Kaufmann, R. B. Myneni, C. J. Tucker, P. E. Kauppi, J. Liski, W. Buermann, V. Alexeyev, and M. K. Hughes. 2003. Remote sensing estimates of boreal and temperate forest woody biomass: carbon pools, sources, and sinks. Remote Sensing of Environment **84**:393-410.

Donoghue, D. N. M. 2002. Remote sensing: environmental change. Progress in Physical Geography **26**:144-151.

Drake, J. B., R. O. Dubayah, D. B. Clark, R. G. Knox, J. B. Blair, M. A. Hofton, R. L. Chazdon, J. F. Weishampel, and S. D. Prince. 2002. Estimation of tropical forest structural characteristics using large-footprint lidar. Remote Sensing of Environment **79**:305-319.

Dubayah, R. O., and J. B. Drake. 2000. Lidar remote sensing for forestry. Journal of Forestry **98**:44-46.

Fahey, T. J., T. G. Siccama, C. T. Driscoll, G. E. Likens, J. Campbell, C. E. Johnson, J. J. Battles, J. D. Aber, J. J. Cole, M. C. Fisk, P. M. Groffman, S. P. Hamburg, R. T. Holmes, P. A. Schwarz, and R. D. Yanai. 2005. The biogeochemistry of carbon at Hubbard Brook. Biogeochemistry **75**:109-176.

Foley, J. A., I. C. Prentice, N. Ramankutty, S. Levis, D. Pollard, S. Sitch, and A. Haxeltine. 1996. An integrated biosphere model of land surface processes, terrestrial carbon balance, and vegetation dynamics. Global Biogeochemical Cycles **10**:603-628.

Friend, A. D., A. K. Stevens, R. G. Knox, and M. G. R. Cannell. 1997. A process-based, terrestrial biosphere model of ecosystem dynamics (Hybrid v3.0). Ecological Modelling **95**:249-287.

Gerhardt, F., and D. R. Foster. 2002. Physiographical and historical effects on forest vegetation in central New England, USA. Journal of Biogeography **29**:1421-1437.

Gillespie, A. J. R. 1999. Rationale for a National Annual Forest Inventory program. Journal of Forestry **97**:16-20.

Goodale, C. L., M. J. Apps, R. A. Birdsey, C. B. Field, L. S. Heath, R. A. Houghton, J. C. Jenkins, G. H. Kohlmaier, W. Kurz, S. R. Liu, G. J. Nabuurs, S. Nilsson, and A. Z. Shvidenko. 2002. Forest carbon sinks in the Northern Hemisphere. Ecological Applications **12**:891-899.

Hurtt, G. C., R. Dubayah, J. Drake, P. R. Moorcroft, S. W. Pacala, J. B. Blair, and M. G. Fearon. 2004. Beyond potential vegetation: combining lidar data and a height-structured model for carbon studies. Ecological Applications **14**:873-883.

Hurtt, G. C., P. R. Moorcroft, S. W. Pacala, and S. A. Levin. 1998. Terrestrial models and global change: challenges for the future. Global Change Biology **4**:581-590.

Hurtt, G. C., S. W. Pacala, P. R. Moorcroft, J. Caspersen, E. Shevliakova, R. A. Houghton, and B. Moore. 2002. Projecting the future of the US carbon sink. Proceedings of the National Academy of Sciences of the United States of America **99**:1389-1394.

Joshi, A. B., D. R. Vann, A. H. Johnson, and E. K. Miller. 2003. Nitrogen availability and forest productivity along a climosequence on Whiteface Mountain, New York. Canadian Journal of Forest Research-Revue Canadienne De Recherche Forestiere **33**:1880-1891.

Kasischke, E. S., J. M. Melack, and M. C. Dobson. 1997. The use of imaging radars for ecological applications - A review. Remote Sensing of

Environment **59**:141-156.

Lefsky, M. A., W. B. Cohen, D. J. Harding, G. G. Parker, S. A. Acker, and S. T. Gower. 2002a. Lidar remote sensing of above-ground biomass in three biomes. Global Ecology and Biogeography **11**:393-399.

Lefsky, M. A., W. B. Cohen, G. G. Parker, and D. J. Harding. 2002b. Lidar remote sensing for ecosystem studies. Bioscience **52**:19-30.

Likens, G. E., and F. H. Bormann. 1995. Biogeochemistry of a forested ecosystem. 2nd edition. Springer-Verlag, New York.

Lucas, N. S., and P. J. Curran. 1999. Forest ecosystem simulation modelling: the role of remote sensing. Progress in Physical Geography **23**:391-423.

Melillo, J. M., A. D. Mcguire, D. W. Kicklighter, B. Moore, C. J. Vorosmarty, and A. L. Schloss. 1993. Global Climate-Change and Terrestrial Net Primary Production. Nature **363**:234-240.

Merrens, E. J., and D. R. Peart. 1992. Effects of Hurricane Damage on Individual Growth and Stand Structure in a Hardwood Forest in New-Hampshire, USA. Journal of Ecology **80**:787-795.

Moorcroft, P. R., G. C. Hurtt, and S. W. Pacala. 2001. A method for scaling vegetation dynamics: The ecosystem demography model (ED). Ecological Monographs **71**:557-585.

Ollinger, S. V., J. D. Aber, A. C. Federer, G. M. Lovett, and J. M. Ellis. 1995. Modeling physical and chemical climate of the northeastern United States for a geographic information system. U.S. Department of Agriculture, Forest Service, Northeastern Forest Experiment Station, Radnor, PA.

Pacala, S. W., C. D. Canham, J. Saponara, J. A. Silander, R. K. Kobe, and E. Ribbens. 1996. Forest models defined by field measurements: Estimation, error analysis and dynamics. Ecological Monographs **66**:1-43.

Pacala, S. W., C. D. Canham, and J. A. Silander. 1993. Forest Models Defined by Field-Measurements .1. The Design of a Northeastern Forest Simulator. Canadian Journal of Forest Research-Revue Canadienne De Recherche Forestiere **23**:1980-1988.

Patenaude, G., R. A. Hill, R. Milne, D. L. A. Gaveau, B. B. J. Briggs, and T. P. Dawson. 2004. Quantifying forest above ground carbon content using LiDAR remote sensing. Remote Sensing of Environment **93**:368-380.

Peart, D. R., C. V. Cogbill, and P. A. Palmiotto. 1992. Effects of Logging History and Hurricane Damage on Canopy Structure in a Northern Hardwoods Forest. Bulletin of the Torrey Botanical Club **119**:29-38.

Peterson, B. E. 2000. Recovery of forest canopy heights using large-footprint lidar. University of Maryland, College Park, College Park, Maryland, USA.

Popescu, S. C., R. H. Wynne, and R. F. Nelson. 2003. Measuring individual tree crown diameter with lidar and assessing its influence on estimating forest volume and biomass. Canadian Journal of Remote Sensing **29**:564-577.

Potter, C. S., E. A. Davidson, S. A. Klooster, D. C. Nepstad, G. H. De Negreiros, and V. Brooks. 1998. Regional application of an ecosystem production model for studies of biogeochemistry in Brazilian Amazonia. Global Change Biology **4**:315-333.

Raich, J. W., E. B. Rastetter, J. M. Melillo, D. W. Kicklighter, P. A. Steudler, B. J. Peterson, A. L. Grace, B. Moore, and C. J. Vorosmarty. 1991. Potential Net Primary Productivity in South-America - Application of a Global-Model. Ecological Applications **1**:399-429.

Ranson, K. J., G. Sun, R. G. Knox, E. R. Levine, J. F. Weishampel, and S. T. Fifer. 2001. Northern forest ecosystem dynamics using coupled models and remote sensing. Remote Sensing of Environment **75**:291-302.

Ranson, K. J., G. Sun, J. F. Weishampel, and R. G. Knox. 1997. Forest biomass from combined ecosystem and radar backscatter modeling. Remote Sensing of Environment **59**:118-133.

Rhoads, A. G., S. P. Hamburg, T. J. Fahey, T. G. Siccama, E. N. Hane, J. Battles, C. Cogbill, J. Randall, and G. Wilson. 2002. Effects of an intense ice storm on the structure of a northern hardwood forest. Canadian Journal of Forest Research-Revue Canadienne De Recherche Forestiere **32**:1763-1775.

Richardson, A. D., X. Lee, and A. J. Friedland. 2004. Microclimatology of treeline spruce-fir forests in mountains of the northeastern United States. Agricultural and Forest Meteorology **125**:53-66.

Schilz, M. 2006. Understanding changes in aboveground biomass and height with elevation at Hubbard Brook Experimental Forest. University of New Hampshire, Durham, New Hampshire, USA.

Schwarz, P. A., T. J. Fahey, and C. E. McCulloch. 2003. Factors controlling spatial variation of tree species abundance in a forested landscape. Ecology **84**:1862-1878.

Shugart, H. H. 1984. A theory of forest dynamics : the ecological implications of forest succession models. Springer-Verlag, New York.

Shugart, H. H., and D. C. West. 1977. Development of an Appalachian Deciduous Forest Succession Model and Its Application to Assessment of Impact of Chestnut Blight. Journal of Environmental Management **5**:161-179.

Siccama, T. G., S. P. Hamburg, M. A. Arthur, R. D. Yanai, F. H. Bormann, and G. E. Likens. 1994. Corrections to Allometric Equations and Plant-Tissue Chemistry for Hubbard-Brook-Experimental-Forest. Ecology **75**:246-248.

Singh, S. P., B. S. Adhikari, and D. B. Zobel. 1994. Biomass, Productivity, Leaf Longevity, and Forest Structure in the Central Himalaya. Ecological Monographs **64**:401-421.

Turner, D. P., S. V. Ollinger, and J. S. Kimball. 2004. Integrating remote sensing and ecosystem process models for landscape- to regional-scale analysis of the carbon cycle. Bioscience **54**:573-584.

van Aardt, J. A. N., R. H. Wynne, and R. G. Oderwald. 2006. Forest volume and biomass estimation using small-footprint lidar-distributional parameters on a per-segment basis. Forest Science **52**:636-649.

Whittaker, R. H., F. H. Bormann, G. E. Likens, and T. G. Siccama. 1974. Hubbard Brook Ecosystem Study - Forest Biomass and Production. Ecological Monographs **44**:233-252.

Whittaker, R. H., G. E. Likens, F. H. Bormann, J. S. Eaton, and T. G. Siccama. 1979. Hubbard Brook Ecosystem Study - Forest Nutrient Cycling and Element Behavior. Ecology **60**:203-220.

Whittaker, R. H., and W. A. Niering. 1975. Vegetation of Santa Catalina Mountains, Arizona .5. Biomass, Production, and Diversity Along Elevation Gradient. Ecology **56**:771-790.

Zwally, H. J., B. Schutz, W. Abdalati, J. Abshire, C. Bentley, A. Brenner, J. Bufton, J. Dezio, D. Hancock, D. Harding, T. Herring, B. Minster, K. Quinn, S. Palm, J. Spinhirne, and R. Thomas. 2002. ICESat's laser measurements of polar ice, atmosphere, ocean, and land. Journal of Geodynamics **34**:405-445.